Available online at www.sciencedirect.com
SCIENCE DIRECT®
Journal of Organometallic Chemistry 687 (2003) 57–68
Journal of Organometallic Chemistry
www.elsevier.com/locate/jorganchem

Mono- and binuclear bipyridyl derivatives of the $Mo(\eta^3\text{-}C_3H_5)(CO)_2$ fragment: structural studies and fluxionality in solution

Pedro M.F.J. Costa [a], Márcia Mora [a], Maria José Calhorda [a,b,*], Vitor Félix [c], Paula Ferreira [b], Michael G.B. Drew [d], Hubert Wadepohl [e]

[a] *Instituto de Tecnologia Química e Biológica (ITQB), Av. da República, EAN, Apt 127, 2781-901 Oeiras, Portugal*
[b] *Departamento de Química e Bioquímica, Faculdade de Ciências da Universidade de Lisboa, 1749-016 Lisboa, Portugal*
[c] *Departamento de Química, Universidade de Aveiro, CICECO, 3810-193 Aveiro, Portugal*
[d] *Department of Chemistry, University of Reading, Whiteknights, Reading RG6 6AD, UK*
[e] *Anorganisch-chemisches Institut der Ruprecht-Karls-Universität, Im Neuenheimer Feld 270, D-69120 Heidelberg, Germany*

Received 10 July 2003; received in revised form 1 August 2003; accepted 13 August 2003

Abstract

New mono- and binuclear complexes of the $Mo(\eta^3\text{-}C_3H_5)(CO)_2$ fragment, containing bipyridyl ligands (2,2′-bpy, 4,4′-Me_2-2,2′-bpy) as chelates, and mono- (4-CNpy, 4-Mepy, NCMe, Br) or bidentate nitrogen ligands (4,4′-bpy, bipyridylethylene, pyrazine) as terminal or bridging ligands, respectively, were prepared. The binuclear complex $[\{Mo(\eta^3\text{-}C_3H_5)(CO)_2(2,2'\text{-bpy})\}_2(\mu\text{-}4,4'\text{-bpy})][PF_6]_2$ (**2**) was shown by X-ray diffraction to assemble in the crystal forming large channels with a rectangular section. A longer bridge, such as bipyridylethylene, led to a different structure (**3**). 4-CNpy behaved as monodentate ligand (**4**), coordinating through the pyridine nitrogen as a terminal ligand. NMR spectroscopy studies showed that the complexes exhibited a fluxional behavior in solution, the *endo* and *exo* forms of the more symmetrical equatorial isomers being usually present and interconverting in solution. The solid state structures of the complexes revealed a preference for the more symmetrical equatorial isomer, with the two chelate ligands in *trans* positions in the binuclear species. The rings tended to become parallel in the organized crystal.

Keywords: Molybdenum; Allyl complexes; Crystal structures; Bipyridyl complexes; Binuclear complexes

1. Introduction

Organometallic complexes have been widely used as building blocks to design molecular solids [1]. Their versatility over organic precursors lies, among others, in the range of available oxidation states giving rise to different structural preferences and electron count, and in the possibility of modifying the ligands in order to favor intermolecular interactions, from electrostatic interactions, to hydrogen bonds, and weak van der Waals forces. Bridging ligands allow the formation of polynuclear species, where metal communication can be tuned by redox means. Some ligands, such as 4,4′-bpyridyl, have shown their potential in helping to stabilize open structures with channels [2], widening the field of applications.

The well known allyl complex $[Mo(\eta^3\text{-}C_3H_5)(CO)_2(NCMe)_2X]$, where X is a halide [3], has been shown as a useful precursor to prepare mononuclear derivatives, used both as catalysts for polymerization of certain dienes [4] and in organic synthesis for allylic alkylations [5]. These complexes, having the two nitriles replaced by a L–L ligand, for instance, always show a *fac* arrangement of the $\eta^3\text{-}C_3H_5$ and the two CO ligands and can exhibit two isomers, **E** (equatorial) with C_s symmetry and **A** (axial) without symmetry (Scheme 1). Their interconversion processes in solution have been discussed before [6,7].

Binuclear complexes have also been synthesized, containing halide [3c,8] or other bridges [9], or oxalate bridges replacing two nitrile ligands in each precursor molecule [3a].

* Corresponding author. Tel.: +351-21-446-9754; fax: +351-21-441-1277.
E-mail address: mjc@itqb.unl.pt (M.J. Calhorda).

0022-328X/03/$ - see front matter © 2003 Elsevier B.V. All rights reserved.
doi:10.1016/j.jorganchem.2003.08.004

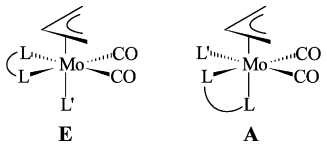

Scheme 1.

In this work, the synthesis of new dimeric species, where a suitable bridging ligand, such as 4,4′-bipyridyl, has replaced X in two units of **1**, was attempted. The effect of changing other coligands and the bridge upon the crystal structures, as well as the dynamic behavior in solution, are discussed.

2. Results and discussion

2.1. Chemical studies

The allyl complex [Mo(η^3-C_3H_5)(CO)$_2$(2,2′-bpy)Br] (**1**) can be used as a convenient source of molybdenum(II) derivatives, because in the presence of Tl[PF_6] and a neutral ligand L a cationic species [Mo(η^3-C_3H_5)(CO)$_2$(2,2′-bpy)L]$^+$ is formed [6]. When L is 4,4′-bipyridyl, in a 1:2 ratio to **1**, the reaction in acetone led, after discarding the TlBr precipitate, to the new binuclear complex [{Mo(η^3-C_3H_5)(CO)$_2$(2,2′-bpy)}$_2$(μ-4,4′-bpy)][PF_6]$_2$ (**2**). The two $\nu_{C\equiv O}$ stretching bands were shifted upon dimer formation to higher frequencies (1952, 1879 cm^{-1}) relative to those of **1** (1929, 1844cm^{-1}), reflecting the cationic nature of the new complex. The structure was unequivocally assigned, according to the single crystal X-ray study, as **EE** in Scheme 2 (see below). The ^{1}H- and ^{13}C-NMR spectra were consistent with the proposed formulation but showed the presence of more than one isomer in solution, indicating a dynamic behavior. There are three possible isomers of this binuclear complex, which contain a *fac* arrangement of the η^3-C_3H_5 and the two CO ligands, with the open face of the allyl eclipsing the carbonyl groups, as depicted in Scheme 2. This arrangement, maximizing back donation to the carbonyls, is preferred [6].

The **EE** isomer exhibits C_s symmetry, **AA** has C_2 symmetry and **EA** is asymmetric. The NMR and MS

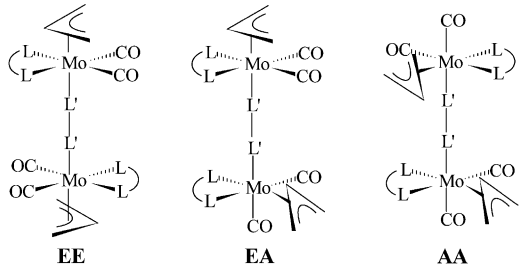

Scheme 2.

data will be discussed below. Other possible isomers with the allyl *trans* to the carbonyls have higher energies [6].

Similar reactions were carried out using other bridging ligands, namely pyrazine, bipyridylethylene (BPE), and 4-cyanopyridine, with the same 1:2 stoichiometry, in order to explore the effect of changing bridge size upon the crystal structure. 4,4′-Me$_2$-2,2′-bpy was tested as a chelate ligand with the same purpose, while the non-bridging 4-Mepy ligand was used for comparison. The binuclear complex [{Mo(η^3-C_3H_5)(CO)$_2$(2,2′-bpy)}$_2$(μ-BPE)][PF_6]$_2$ (**3**), and the mononuclear ones [Mo(η^3-C_3H_5)(CO)$_2$(2,2′-bpy)(4-CNpy)][PF_6] (**4**) and [Mo(η^3-C_3H_5)(CO)$_2$(2,2′-bpy)(4-Mepy)][PF_6] (**5**), were obtained, while the dimer with a pyrazine bridge proved to be too unstable to characterize. The use of the dimethyl substituted bipyridyl ligand as chelate, however, allowed this difficulty to be overcome and complex [{Mo(η^3-C_3H_5)(CO)$_2$(4,4′-Me$_2$-2,2′-bpy)}$_2$(μ-pyrazine)][PF_6]$_2$ (**6**) to be isolated.

The complexes were characterized by elemental analysis, IV spectroscopy, ^{13}C- and ^{1}H-NMR, and mass spectroscopy (see below and Section 4). Single crystal X-ray studies also led to the assignment of the structures of [{Mo(η^3-C_3H_5)(CO)$_2$(2,2′-bpy)}$_2$(μ-BPE)][PF_6]$_2$ (**3**), [Mo(η^3-C_3H_5)(CO)$_2$(2,2′-bpy)(4-CNpy)][PF_6] (**4**), and [Mo(η^3-C_3H_5)(CO)$_2$(2,2′-bpy)(4-Mepy)][PF_6] (**5**), showing the same species to be present in the crystal and in solution. However, the crystals obtained from the slow diffusion of solvent vapor into acetonitrile (the method used for all species), led in the case of [{Mo(η^3-C_3H_5)(CO)$_2$(4,4′-Me$_2$-2,2′-py)}$_2$(μ-pyrazine)][PF_6]$_2$ (**6**), to a mononuclear complex formed by substitution of the bridging pyrazine by acetonitrile, yielding [{Mo(η^3-C_3H_5)(CO)$_2$(4,4′-Me$_2$-2,2′-bpy)(NCMe)][PF_6] (**7**). The related [{Mo(η^3-C_3H_5)(CO)$_2$(4,4′-Me$_2$-2,2′-bpy)Br] (**8**), used as precursor to prepare **6**, was also structurally characterized.

The mass spectra were studied by positive ion field desorption (FD+). In the mass spectrum of complex [{Mo(η^3-C_3H_5)(CO)$_2$(2,2′-bpy)}$_2$(μ-4,4′-bpy)][PF_6]$_2$ (**2**), the dication [{Mo(η^3-C_3H_5)(CO)$_2$(2,2′-bpy)}$_2$(μ-4,4′-bpy)]$^{2+}$ (*m*/*z* 427.5) appears as the base peak. The ions {[{Mo(η^3-C_3H_5)(CO)$_2$(2,2′-bpy)}$_2$(μ-4,4′-bpy)][PF_6]}$^+$ (*m*/*z* 1000) and {[{Mo(η^3-C_3H_5)(CO)$_2$(2,2′-bpy)}$_2$(μ-4,4′-bpy)][PF_6]$_2$}$^+$ (*m*/*z* 1145) are detected. Observed fragments are [Mo(η^3-C_3H_5)(CO)$_2$(2,2′-bpy)]$^+$ (*m*/*z* 507), [Mo(η^3-C_3H_5)(CO)$_2$(2,2′-bpy)]$^+$ (*m*/*z* 351) and 2,2′-bpy$^+$ (*m*/*z* 156). These fragmentation patterns indicate the loss of two counter ions and formation of two monomers, one of them keeping the 4,4′-bpy ligand.

The mononuclear complex [Mo(η^3-C_3H_5)(CO)$_2$(2,2′-bpy)(4-CNpy)][PF_6] (**4**) yields its parent ion at *m*/*z* 455 in the FD+ mass spectrum, accompanied by the fragment due to loss of 4-CNpy. However, the addi-

tional presence of the 4-cyanopyridine bridged dimolybdenum complex is indicated by a weaker peak at *m/z* 947, assigned to $\{[\{Mo(\eta^3\text{-}C_3H_5)(CO)_2(2,2'\text{-bpy})\}_2(\mu\text{-}4CNpy)][PF_6]\}^+$. Complex **5**, $[Mo(\eta^3\text{-}C_3H_5)(CO)_2(2,2'\text{-bpy})(4\text{-Mepy})][PF_6]$, gives a very similar pattern, but, as 4-Mepy cannot behave as a bridge, no dimolybdenum species containing this ligand are detected.

In the FD+ mass spectra of complexes **2**, **4** and **5** a mass pattern centered on *m/z* 717, with an intensity distribution characteristic of two molybdenum atoms, is detected, in addition to the aforementioned peaks. A likely composition is $[\{Mo(\eta^3\text{-}C_3H_5)(CO)_2(2,2'\text{-bpy})\}_2(F)]^+$ (*m/z* 717).

NMR experiments were carried out at 300 K, unless stated differently, but limited solubility of some complexes prevented their carbon spectra from being obtained. Spin–spin coupling and NOE (detected by COSY, TOCSY and NOESY techniques) were used to group the resonances of allyl *syn*, allyl *anti* and allyl *meso* protons (Scheme 3) in sets arising from chemically inequivalent allyl ligands, as well as for the bpy signals. Not all of the expected peaks could always be resolved, owing to the close spacing of many resonances even at 500 MHz. Symmetrical allyl ligands, with a plane of symmetry bisecting the allyl C_3 plane on the NMR time scale, exhibited two doublets for *syn* and *anti*, and a multiplet for the *meta* protons, and usually showed NOE cross peaks between the resonances of the *syn* protons and the low field signals assignable to H-6 of a corresponding 2,2′-bpy. This indicates the molecular substructure **E** (Scheme 1).

Dynamic processes which interconvert various species were detected using 2D-EXSY spectra. The timescale of this kind of dynamic NMR experiment is much slower than those involving changes of lineshapes. Corresponding mixing times in the EXSY experiments, roughly defining the lifetime of the individual species, were set between some hundred milliseconds and several seconds. The molecular species in dynamic equilibrium shall be denoted **I** and **II**. Rotation of the allyl in **E** generates two isomers with symmetric allyls (*endo* and *exo* forms, Scheme 3), which can be assigned as **I** and **II**. Our NOESY spectra do not allow us to give a pairwise assignment of **I** and **II** to *exo* and *endo*, due to the presence of chemical exchange.

The spectra of complex $[Mo(\eta^3\text{-}C_3H_5)(CO)_2(2,2'\text{-bpy})(4\text{-CNpy})][PF_6]$ (**4**) show the resonances of two symmetrical allyl ligands and a complex pattern of

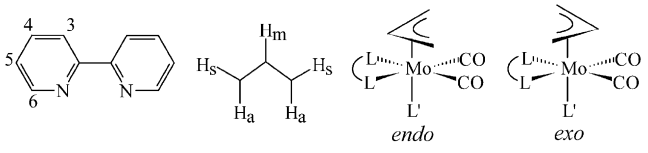

Scheme 3.

proton resonances in the region $7 < \delta < 9.5$, which can be assigned to two inequivalent 2,2′-bpy ligands, but only one set of proton resonances, in a pattern characteristic of an $(AB)_2$ spin system, for the 4-cyanopyridine ligand. The spectra are thus consistent with the presence of the *exo* and *endo* isomers of an **E**-type structure (Schemes 1 and 3) of **4**, slowly interconverting in solution. Only one set of resonances is observed for the cyanopyridine, indicating that the rotational orientation of the allyls is not felt differently. The NMR spectra of the related complex $[Mo(\eta^3\text{-}C_3H_5)(CO)_2(2,2'\text{-bpy})(4\text{-Mepy})][PF_6]$ (**5**), indicate the presence of *three* species in the ratio 1:2:2.8. Two can be assigned to the *exo* and *endo* forms of structure **E**, while the third set of allyl resonances likely corresponds to structure **A**. Extensive overlap of resonances precludes a complete analysis of the spectra.

In the binuclear species, there are more possible species in solution. In an **EE** structure of $[\{Mo(\eta^3\text{-}C_3H_5)(CO)_2(L)\}_2(\mu\text{-}L')]$ (Scheme 2) there are three possible isomers: *exo/exo*, *exo/endo* and *endo/endo* (Scheme 3). As the proton resonances of the bridging ligand L′ are not sensitive to the *exo* or *endo* orientation of any particular allyl system, according to the results of complex **4**, we cannot distinguish between an approximately 1:1 mixture of the more symmetrical *exo/exo* and *endo/endo* isomers, the *exo/endo* species and a mixture of all three. The 500 MHz ^{1}H-NMR spectrum of the binuclear complex $[\{Mo(\eta^3\text{-}C_3H_5)(CO)_2(2,2'\text{-bpy})\}_2(\mu\text{-}4,4'\text{-bpy})][PF_6]_2$ (**2**), shows in the region $7.5 < \delta < 9.2$ three sets of two multiplets each, which can be assigned to three $(AB)_2$ spin systems with an approximate intensity ratio of 4:1:1. 2D NMR techniques allow the identification of the subspectra of three symmetrical 2,2′-bpy ligands, as well as three sets of symmetrical allyl resonances, **I**, **II** and **III** (see Section 4). Using the correlation from NOEs and spin–spin coupling as well as the integrals, the spectra can be explained by the presence of three species: the mononuclear $[Mo(\eta^3\text{-}C_3H_5)(CO)_2(2,2'\text{-bpy})(4,4'\text{-bpy})]^+$ and two isomers of the binuclear $[\{Mo(\eta^3\text{-}C_3H_5)(CO)_2(2,2'\text{-bpy})\}_2(\mu\text{-}4,4'\text{-bpy})]^{2+}$ (**2**).

In the mononuclear complex $[Mo(\eta^3\text{-}C_3H_5)(CO)_2(2,2'\text{-bpy})(4,4'\text{-bpy})]^+$, the terminal monodentate 4,4′-bpy ligand is asymmetric and hence the protons of this ligand form two $(AB)_2$ spin systems, consisting of a total of four multiplets. In contrast, only one $(AB)_2$ pattern is due to a bridging 4,4′-bpy ligand. For the binuclear species, the usual slow exchange between the allyls **I** and **II** is observed in the EXSY experiment at 300 K. A faster dynamic process can be slowed down on the T_2 NMR timescale a low temperature. This process involves only allyl **I**, which becomes asymmetric on cooling, giving rise to two *anti*, two *syn* and one *meso* resonance at low temperature. Changes are also obvious with the bpy resonances. Unfortu-

nately, due to solubility problems, which became unsurmountable below −40 °C, well resolved limiting spectra could not be obtained.

These observations are consistent with the presence of the two *exo* and *endo* isomers of an **EE**-type structure of **2** at room temperature, which slowly interconvert in solution. On cooling, one of the allyls (i.e. either the *exo* or *endo*) in the binuclear isomers moves from its position *trans* to the bridging 4,4′-bpy into a *cis* position (isomer **E** to isomer **A** in Scheme 1). Being still away from the low temperature limit, we cannot draw further conclusions about the low temperature structure of **2**. Interestingly, the mononuclear complex $[Mo(\eta^3\text{-}C_3H_5)(CO)_2(2,2'\text{-bpy})(4,4'\text{-bpy})]^+$ seems to exist as only one isomer, structural type **E**.

The binuclear complex $[\{Mo(\eta^3\text{-}C_3H_5)(CO)_2(4,4'\text{-}Me_2\text{-}2,2'\text{-bpy})\}_2(\mu\text{-pyrazine})][PF_6]_2$ (**6**) behaves similarly at 304 K, showing the resonances of two symmetrically bonded allyl groups, two singlets due to methyl groups, and two sets of three resonances, which can be assigned to the ring protons of the 4,4′-Me_2-2,2′-bpy ligands. One singlet at $\delta = 8.7$arises from the equivalent protons of the bridging pyrazine ligand. This assignment was consistent with NOE and exchange cross peaks and can be explained by two exchanging isomers of an **EE**-type structure of **6**.

2.2. Crystal structures of complexes [{Mo(η³-C₃H₅)(CO)₂(2,2′-bpy)}₂(μ-4,4′-bpy)][PF₆]₂ (2), [{Mo(η³-C₃H₅)(CO)₂(2,2′-bpy)}₂(μ-BPE)][PF₆]₂ (3), [Mo(η³-C₃H₅)(CO)₂(2,2′-bpy)(4-CNpy)][PF₆] (4), [Mo(η³-C₃H₅)(CO)₂(2,2′-bpy)(4-Mepy)][PF₆] (5), [Mo(η³-C₃H₅)(CO)₂(4,4′-Me₂-2,2′-bpy)(NCMe)][PF₆] (7), and [Mo(η³-C₃H₅)(CO)₂(4,4′-Me₂-2,2′-bpy)Br] (8)

The solid state structures of PF_6 salts of two binuclear complexes $[\{Mo(\eta^3\text{-}C_3H_5)(CO)_2(2,2'\text{-bpy})\}_2(\mu\text{-L})]^{2+}$ (L = 4,4′-bpy, **2**; L = BPE, **3**) and of four mononuclear related species $[Mo(\eta^3\text{-}C_3H_5)(CO)_2(2,2'\text{-bpy})L]^+$ (L = 4-CN-py, **4**; L = 4-Mepy, **5**) and $[Mo(\eta^3\text{-}C_3H_5)(CO)_2(4,4'\text{-}Me_2\text{-}2,2'\text{-bpy})L]^{n+}$ (L = NCME and $n = 1$, **7**; L = Br and $n = 0$, **8**), were determined by single crystal X-ray diffraction (XRD). The crystals of **4**, **5**, and **7** displayed weak diffraction patterns and consequently slightly higher values than usual for the final *R*-values were obtained, as well as for the standard deviations of the molecular dimensions. However, the structures of these three complexes were determined unequivocally, providing a detailed characterization of the molybdenum(II) coordination spheres. On the other hand, this set of six complexes allows a broad discussion of the conformational features associated with the apparently flexible $Mo(\eta^3\text{-}C_3H_5)(CO)_2$ bipyridyl derivatives. For comparison purposes the structures will be discussed together.

The unit cells of mononuclear species **4**, **5**, and **7** are built up from asymmetric units composed of one complex cation $[Mo(\eta^3\text{-}C_3H_5)(CO)_2(bpy)L]^+$ (bpy stands here for 2,2′-bpy and 4,4′-Me_2-2,2′-bpy) and one PF_6^- counter ion, both in general crystallographic positions. In the crystal structures of **7** and **5**, the PF_6^- anions are disordered over two positions. In addition, the asymmetric unit of **5** contains a cocrystallized water molecule with an occupancy of 0.5. The crystal structure of **8** consist of discrete molecules of $[Mo(\eta^3\text{-}C_3H_5)(CO)_2(4,4'\text{-}Me_2\text{-}2,2'\text{-bpy})Br]$ (**8**). ORTEP diagrams of the monocationic complexes **4**, **5**, **7** showing the molecular structures and the crystallographic labeling scheme adopted, are presented in Figs. 1–3, respectively. The molecular structure of the neutral complex **8** is presented in Fig. 4. Selected distances and angles are given in Table 1.

In the asymmetric unit of the binuclear complex **2** there is one half independent $[\{Mo(\eta^3\text{-}C_3H_5)(CO)_2(2,2'\text{-bpy})\}_2(\mu\text{-}4,4'\text{-bpy})]^{2+}$ dication and one PF_6^- anion, while the asymmetric unit of $[\{Mo(\eta^3\text{-}C_3H_5)(CO)_2(2,2'\text{-bpy})\}_2(\mu\text{-BPE})][PF_6]_2$ (**3**) comprises two independent half cations, two PF_6^- anions and two solvent molecules. These consist of one acetonitrile and one water molecules, which is disordered over two positions. In the two independent molecules, the ligands adopt identical dispositions around the metal center and the bond lengths and angles are also identical within the standard limits. Therefore, in this discussion, average values for the structural parameters will be used, unless otherwise stated. Molecular ORTEP diagrams of the

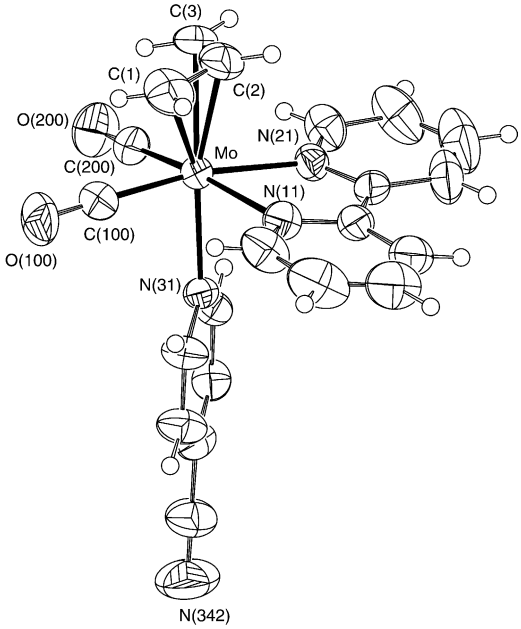

Fig. 1. ORTEP view of $[Mo(\eta^3\text{-}C_3H_5)(CO)_2(2,2'\text{-bpy})(4\text{-CNpy})]^+$ (**4**) with thermal ellipsoids drawn at 30% of probability level, showing the overall structure and the atomic crystallographic atomic notation scheme adopted.

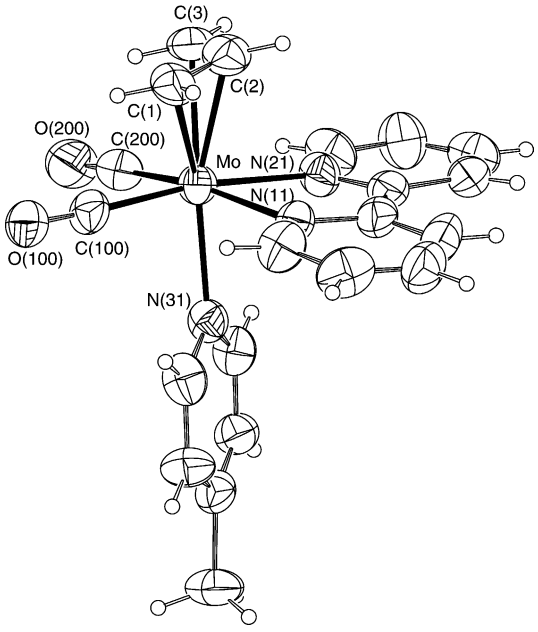

Fig. 2. ORTEP view of $[Mo(\eta^3\text{-}C_3H_5)(CO)_2(2,2'\text{-bpy})(4\text{-Mepy})]^+$ (**5**). Details are given in Fig. 1.

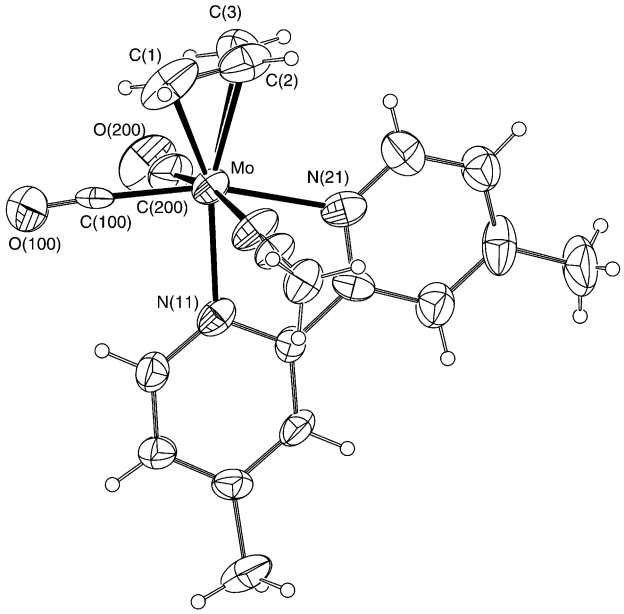

Fig. 3. ORTEP view of $[Mo(\eta^3\text{-}C_3H_5)(CO)_2(4,4'\text{-}Me_2\text{-}2,2'\text{-bpy})(NCMe)]^+$ (**7**). Details are given in Fig. 1.

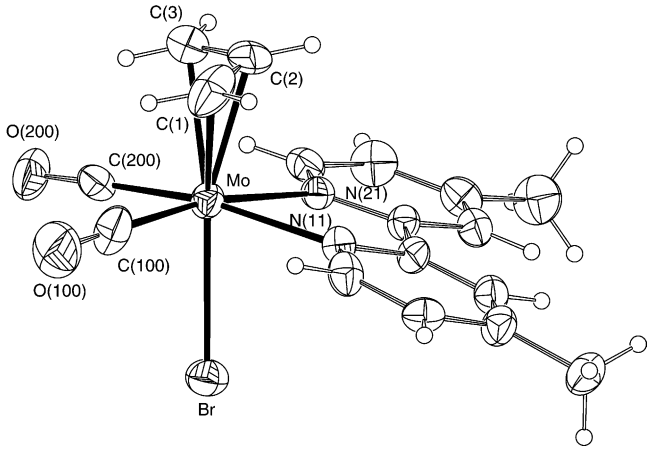

Fig. 4. ORTEP view of $[Mo(\eta^3\text{-}C_3H_5)(CO)_2(4,4'\text{-}Me_2\text{-}2,2'\text{-bpy})Br]$ (**8**). Details are given in Fig. 1.

Table 1
Selected bond lengths (Å) and angles (°) in the molybdenum coordination sphere of the mononuclear complexes **4**–**5** and **7**–**8**

*$[Mo(\eta^3\text{-}C_3H_5)(CO)_2(2,2'\text{-bpy})(4\text{-CNpy})]^+$ (**4**)*			
Mo–N(31)	2.26(1)		
Mo–N(11)	2.24(1)	Mo–N(21)	2.25(1)
Mo–C(100)	1.96(1)	Mo–C(200)	1.96(1)
Mo–C(1)	2.34(1)	Mo–C(2)	2.22(1)
Mo–C(3)	2.36(1)		
N(11)–Mo–N(21)	72.8(3)		
*$[Mo(\eta^3\text{-}C_3H_5)(CO)_2(2,2'\text{-bpy})(4\text{-Mepy})]^+$ (**5**)*			
Mo–N(31)	2.25(1)	Mo–N(11)	2.22(1)
Mo–N(21)	2.23(1)	Mo–C(100)	2.00(1)
Mo–C(200)	1.97(2)	Mo–C(1)	2.35(2)
Mo–C(2)	2.23(2)	Mo–C(3)	2.33(1)
N(11)–Mo–N(21)	73.7(4)		
*$[Mo(\eta^3\text{-}C_3H_5)(CO)_2(4,4'\text{-}Me_2\text{-}2,2'\text{-bpy})(NCMe)]^+$ (**7**)*			
Mo–N(301)	2.17(1)		
Mo–N(11)	2.24(1)	Mo–N(21)	2.32(1)
Mo–C(100)	1.98(1)	Mo–C(200)	1.92(2)
Mo–C(1)	2.23(2)	Mo–C(2)	2.26(2)
Mo–C(3)	2.41(1)		
N(11)–Mo–N(21)	76.2(4)		
*$[Mo(\eta^3\text{-}C_3H_5)(CO)_2(4,4'\text{-}Me_2\text{-}2,2'\text{-bpy})Br]$ (**8**)*			
Mo–Br	2.65(1)		
Mo–N(11)	2.24(1)	Mo–N(21)	2.26(1)
Mo–C(100)	1.94(1)	Mo–C(200)	1.94(1)
Mo–C(1)	2.34(1)	Mo–C(2)	2.23(1)
Mo–C(3)	2.34(1)		
N(11)–Mo–N(21)	73.1(3)		

binuclear cations **2** and **3**, including the crystallographic atomic notation scheme, are presented in Figs. 5 and 6, respectively. Selected distances and angles are given in Table 2.

Both species contain a crystallographic inversion center, which is located in the middle of the central C–C bond of the bridge (4,4′-bpy bridge in **2** and BPE in **3**). Thus, in both complexes, there is a dihedral angle of 180° between chelate bpy rings, and the two $Mo(\eta^3\text{-}C_3H_5)(CO)_2(bpy)$ fragments are in a centrosymmetric arrangement. The planarity of the bridging ligands will in principle favor the electronic communication between the two molybdenum centers through the π systems of the 4,4′-bpy or BPE bridges. Indeed, the central C–C distance (1.45(2) Å) in **2** is slightly shorter than the typical value of a C–C single bond, suggesting the existence of some delocalization within the 4,4′-bpy ligand. In complex **3**, the values the C=C bond distances found for the two independent molecules (1.34(4) and

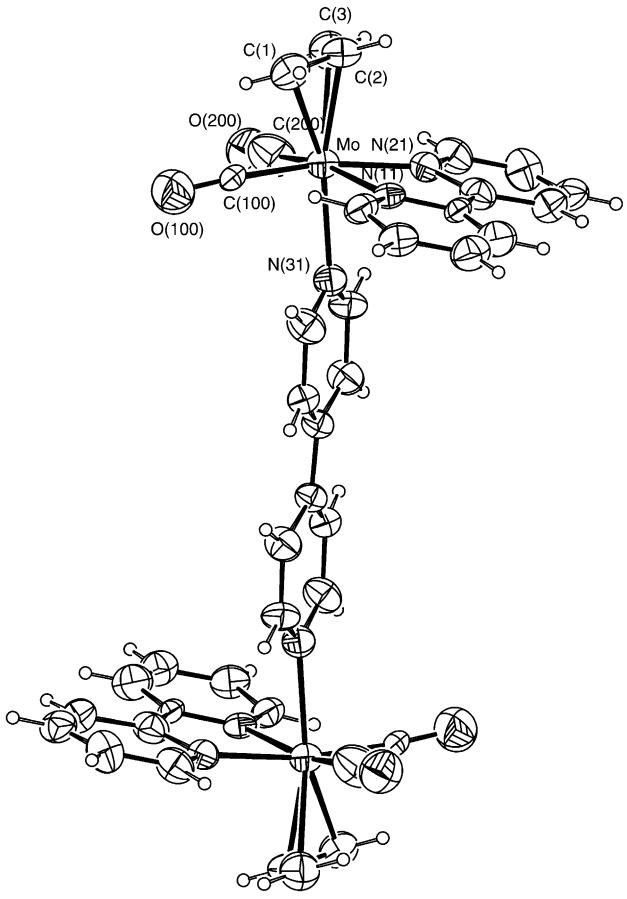

Fig. 5. ORTEP view of $[\{Mo(\eta^3\text{-}C_3H_5)(CO)_2(2,2'\text{-bpy})\}_2(\mu\text{-}4,4'\text{-bpy})]^{2+}$ (**2**). Details are given in Fig. 1.

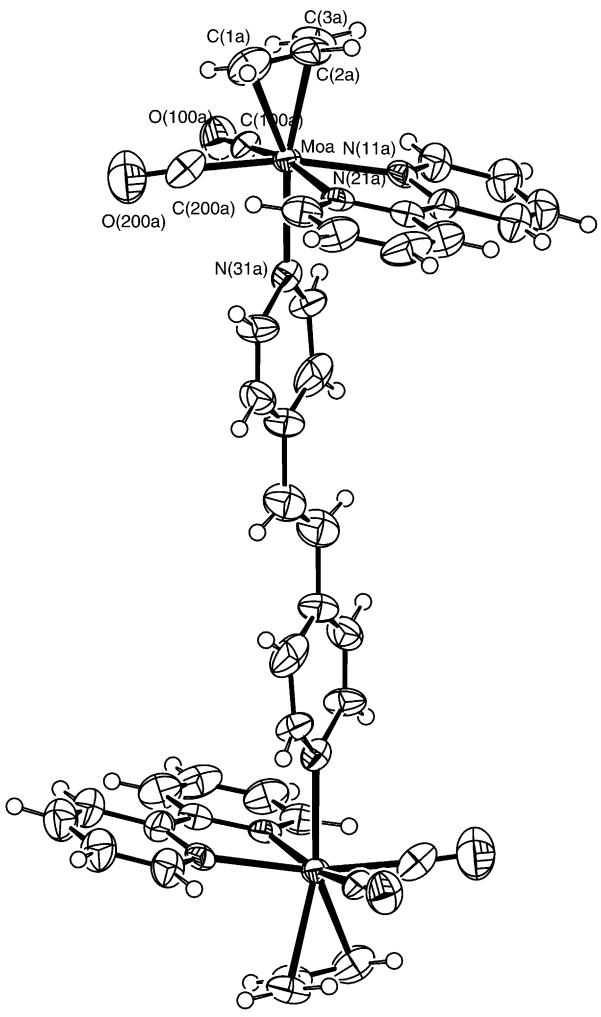

Fig. 6. ORTEP view of $[\{Mo(\eta^3\text{-}C_3H_5)(CO)_2(2,2'\text{-bpy})\}_2(\mu\text{-BPE})]^{2+}$ (**3**). Details are given in Fig. 1.

1.21(4) Å) are consistent with the presence of an isolated carbon–carbon double bond. The two molybdenum centers are separated by long distances of 11.72(1) Å and 13.96(1) Å, reflecting the length of the 4,4′-bpy and BPE spacers, respectively, between the two $Mo(\eta^3\text{-}C_3H_5)(CO)_2(bpy)$ moieties.

The selected molecular dimensions given in Table 1 for complexes **2**–**5** and **7** indicate, in all of them, a pseudo octahedral coordination environment of the molybdenum centers, the centroid of the η^3-allyl ligand and two carbonyl groups determining a *fac* arrangement. Furthermore, in the solid sate, the η^3-allyl ligands always exhibit the usual *endo* conformation with the open side eclipsing the two carbonyl groups. From the comparison of the ORTEP views of the five cationic species, it is clear that the chelation of the bipyridyl ligand can occur in two different sites of the metal coordination sphere and two different geometric arrangements are thus observed (see Scheme 1). In cations **2**–**5**, the carbon atoms from the two carbonyl groups and the two nitrogens of the bpy ligand are on the equatorial co-ordination plane. The axial position opposite the allyl ligand is occupied by bromine in **8** and a nitrogen donor, from 4-CN-py in **4**, or from 4-Mepy in **5**. The related complex $[Mo(\eta^3\text{-}C_3H_5)(CO)_2(2,2'\text{-bpy})(py)][BF_6]$, containing pyridine, also exhibits the same arrangement, the Mo–N distances being comparable, though slightly longer [10]. This type of structure is also observed in the dicationic species **2** and **3**, in which the axial position is fulfilled with a nitrogen donor, but belonging to the bridged ligand. By contrast, in **7**, the monodentate nitrogen donor, acetonitrile, occupies one equatorial position, leaving the axial site for the remaining nitrogen of bpy. Both types of stereochemistry described are quite common and have been found in the solid state before for related $Mo(\eta^3\text{-ally})(CO)_2$ polypyridyl derivatives [6]. The presence of certain ligands in the molybdenum(II) co-ordination sphere can determine the structural preference for one of two possible isomers. However, the complex cation **7** and the neutral species **8** have isomeric structures, suggesting that the geometric arrangement of the ligands around the metal center can be also affected by electronic and/or crystal packing effects.

Table 2
Selected bond lengths (Å) and angles (°) in the molybdenum coordination spheres of the dinuclear cations **2** and **3**

*[{Mo(η³-C₃H₅)(CO)₂(2,2′-bpy)}₂(μ-4,4′-bpy)]²⁺ (**2**)*			
Mo–N(31)	2.29(1)		
Mo–N(11)	2.27(1)	Mo–N(21)	2.09(1)
Mo–C(100)	1.88(1)	Mo–C(200)	2.09(1)
Mo–C(1)	2.40(2)	Mo–C(2)	2.24(1)
Mo–C(3)	2.31(2)	C(34)–C(34_a)[a]	1.45(1)
N(11)–Mo–N(21)	73.6(3)		
*[{Mo(η³-C₃H₅)(CO)₂(2,2′-bpy)}₂(μ-BPE)]²⁺ **3***			
Molecule **A**			
Mo–N(31)	2.24(1)		
Mo–N(11)	2.26(1)	Mo–N(21)	2.23(1)
Mo–C(100)	1.96(2)	Mo–C(200)	1.94(2)
Mo–C(1)	2.33(2)	Mo–C(2)	2.23(2)
Mo–C(3)	2.39(2)	C(37)–C(37_a)[a]	1.21(4)
N(11)–Mo–N(21)	72.3(4)		
*Molecule **B***			
Mo–N(31)	2.26(1)		
Mo–N(11)	2.29(1)	Mo–N(21)	2.24(1)
Mo–C(100)	1.97(2)	Mo–C(200)	1.93(2)
Mo–C(1)	2.35(2)	Mo–C(2)	2.26(2)
Mo–C(3)	2.32(2)	C(37)–C(37_a)[a]	1.34(4)
N(11)–Mo–N(21)	73.2(5)		

[a] $2-x$, $1-y$, $-z$ and $-x$, $2-y$, $1-z$ are the symmetry operations used to generate equivalent atoms in complexes **2** and **3** respectively.

In all complexes, the bipyridyl ligand is slightly tilted with the dihedral angle between the two pyridine rings ranging from 3.6(8)° in **2** to 8.0(8)° in **7**. Furthermore, in complex **8** the tilt angle is only 4.3(6)°, indicating that the presence of two methyl groups on the bpy skeleton does not perturb the value of this parameter. In these complexes, the chelate angles of the bpy ligand around molybdenum fall in a narrow range 72.2(4)–76.2(4)°. As would be expected, the values of the bite angle are dictated by the stereoelectronic demands of the bpy skeleton. All distances and angles listed in Table 1 compare well with those found for related Mo(II)(η³-allyl)(CO)₂bpy complexes [6,10]. The molecular assembling of the $[\{Mo(\eta^3\text{-}C_3H_5)(CO)_2(2,2'\text{-bpy})\}_2(\mu\text{-}4,4'\text{-bpy})]^{2+}$ cations and PF_6^- counter-ions (complex **2**) results in the most interesting crystal packing within this group, as shown by the view down the crystallographic plane [100] presented in Fig. 7. The cations and the anions are aggregated, sheathing open channels running along the *a* crystallographic axis. This arrangement is stabilized by C–H···F hydrogen bonds, between cation and anion, involving two independent interactions C(15)–H(15)···F(5) $[1+x, y, z]$ and C(25)–H(25)···F(4) $[1+x, y, z]$ with H···F distances of 2.14 and 2.44 Å and C–H···F angles of 152.5 and 151.2°, respectively.

Thermogravimetric (TG) and differential scanning calorimetry (DSC) curves were measured in order to investigate the mass loss and the thermodynamic features of complex $[\{Mo(\eta^3\text{-}C_3H_5)(CO)_2(2,2'\text{-bpy})\}_2(\mu\text{-}4,4'\text{-bpy})][PF_6]_2$ (**2**). The TG analysis shows a slow mass loss between the room temperature and 90 °C, which can be assigned to the release of some solvent molecules of the sample. Between 90 °C and 170 °C a second stage of mass loss occurs with ca. of 3.05% mass loss. This is probably due to the loss of solvent molecules (equivalent to 1.95 molecules of water crystallization), which may occupy the open channels of the crystal structure (Fig. 7), but could not be located in the final structure refinement. From the DSC curve it is possible to observe an exothermic peak at this range of temperature that can indicate some changes in the sample different from simple dehydration. Powder XRD indicated the same structure to be present in the temperature range between 25 and 200 °C.

3. Conclusions

The new binuclear complex $[\{Mo(\eta^3\text{-}C_3H_5)(CO)_2(2,2'\text{-bpy})\}_2(\mu\text{-}4,4'\text{-bpy})][PF_6]_2$ (**2**) exhibits an interesting structure with large open channels (Fig. 7), which might be occupied by small molecules. This is consistent with thermogravimetric studies, which also showed that the solid state structure was apparently kept in a relatively wide range of temperatures. NMR spectroscopy studies revealed for the mononuclear complexes of 4-CNpy, at room temperature, the interconverting *endo* and *exo* isomers of the symmetrical equatorial structure **E**. In the case of Mepy, this behavior was also observed. In addition, the asymmetrical structure **A** is also present. The binuclear species offer more possibilities. However, for complex **2**, only the *endo* and *exo* isomers of the **EE** structure (Scheme 3) were observed at room temperature, along with a mononuclear species with terminal 4,4′-bpy. Structural characterization by single crystal XRD revealed that the allyl group eclipses the carbonyl ligands, the three retaining a *fac* arrangement, and the axial isomer is preferred in all cases, except for complex $[Mo(\eta^3\text{-}C_3H_5)(CO)_2(4,4'\text{-}Me_2\text{-}2,2'\text{-bpy})(NCMe)][PF_6]$ (**7**), where a nitrile ligand is present. This suggests that the most stable isomer detected in solution (since complex **7** was only characterized as a solid) should be the *endo* equatorial one (**E**). In most examples studied, this isomer is indeed the most stable one [6], although there are exceptions and a full rationalization of the structural preferences is not yet available.

4. Experimental

4.1. Synthesis

Commercially available reagents and all solvents were purchased from standard chemical suppliers. All sol-

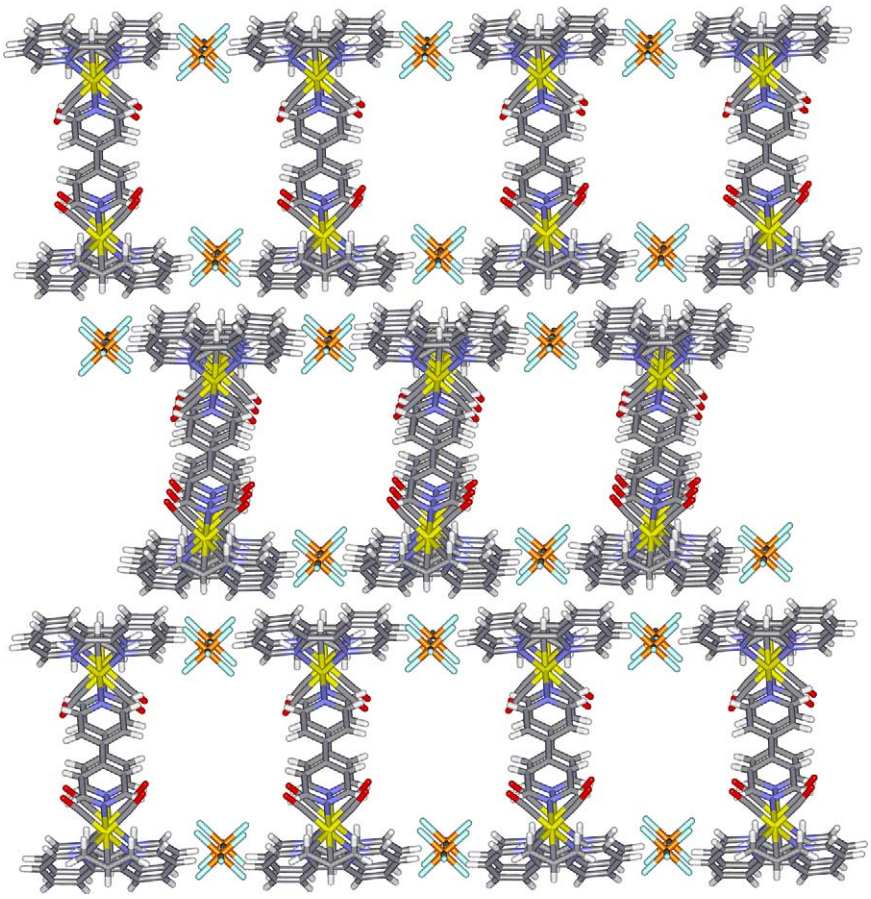

Fig. 7. Crystal packing diagram [{Mo(η^3-C_3H_5)$(CO)_2$(2,2′-bpy)}$_2$(μ-4,4′-bpy)][PF_6]$_2$ (**2**) along the **a** crystallographic axis, showing the open channels.

vents were used without further purification except MeCN (dried over CaH_2), CH_2Cl_2 (dried over CaH_2), and THF, which was distilled over sodium/benzophenone ketyl and used immediately. [Mo(η^3-C_3H_5)$(CO)_2(NCMe)_2$Br] [3] and [Mo(η^3-C_3H_5)$(CO)_2$(2,2′-bpy)Br] [6] were prepared as described in the literature.

Mass spectra were obtained in the positive ion field desorption mode with a JEOL JMS-700 instrument. NMR spectra were recorded on Bruker Avance DRX-200 (200 MHz), AMX-300 (300 MHz) and Avance DRX-500 (500 MHz) spectrometers in acetone-d_6 (δ 2.04), CD_3CN (δ 1.93) and CD_3OD (δ 4.78 and 3.30). Where applicable, the various NMR distinguishable isomers are denoted I, II and III. We thank Z.M. Tavares and M.C. Almeida (ITQB) for elemental analyses. The IR spectra were recorded on a Unicam Mattson 7000 FTIR spectrometer. Samples were run as KBr pellets. Thermogravimetric (TGA) and DSC curves were measured with a Shimadzu TGA-50 analyzer and a Shimadzu DSC-50 analyzer, respectively. The samples were heated under nitrogen at a rate of 5 °C min^{-1}. Powder XRD data were collected on a Philips X'pert MPD diffractometer using Cu–K_α radiation with a curved graphite monochromator and a proportional detector. Data were collected at variable temperature between 3 and 60°, in 2θ with a step size of 0.05°and a count time of 2 s/step.

4.2. Synthesis of [{Mo(CO)$_2$(η^3-C_3H_5)(2,2′-bpy)}$_2$(μ-4,4′-bpy)][PF_6]$_2$ (**2**)

A suspension of [Mo(η^3-C_3H_5)$(CO)_2$(2,2′-bpy)Br] (0.429 g, 1 mmol), Tl[PF_6] (0.349 g, 1 mmol) and 4,4′-bpy (0.078 g, 0.5 mmol) in acetone (20 ml) was refluxed under nitrogen during 5 h. The orange solution was filtered and the TlBr precipitate was washed several times with small amounts of acetone until it became white. The solution was evaporated under vacuum until dryness and was washed three times with ether. The precipitate was recrystallized from CH_2Cl_2–ether. Single crystals suitable for XRD were obtained by diffusion of ether into a concentrated CH_2Cl_2 solution of the complex.

Anal. Calc: C, 41.97; H, 2.99; N, 7.34. Found: C, 41.19; H, 2.85; N, 7.44%.

IR (KBr, cm^{-1}): 1952, 1879 ($\nu_{C\equiv O}$).

^{1}H-NMR (CD_3CN, 500 MHz), δ: 1.58 (d, *anti*-I), 1.65 (d, *anti*-II), 1.81 (*anti*-III), 3.24 (m, *meso*-II), 3.44 (d+m, *syn*-B+*meso*-III), 3.58 (d, *syn*-III), 3.61 (br, *syn*-I), 4.05 (m, *meso*-I), 7.52 (m[a], 4,4′-bpy), 7.56 (m[a], 4,4′-bpy), 7.64 (ddd, 2,2′-bipy H-5), 7.66 (m[a], 4,4′-bpy), 7.74 (ddd, 2,2′-bpy H-5), 7.77 (m, 2,2′-bpy H-5), 8.14 (td, 2,2′-bpy H-4), 8.17 (td, 2,2′-bpy H-4), 8.21 (t, 2,2′-bpy H-4), 8.25 (d, 2,2′-bpy H-3), 8.26 (m[a], 4,4′-bpy), 8.32 (d, 2,2′-bpy H-3), 8.40 (d, 2,2′-bpy H-3), 8.66 (m[a], 4,4′-bpy), 8.69 (m[a], 4,4′-bpy), 8.86 (dm, 2,2′-bpy H-6), 9.1 (br, 2,2′-bpy H-6), 9.16 (dm, 2,2′-bpy H-6); [a] part of a $(AB)_2$ system.

4.3. Synthesis of [{Mo(η^3-C_3H_5)(CO)$_2$(2,2′-bpy)}$_2$(μ-BPE)][PF_6]$_2$ (3)

A suspension of [Mo(η^3-C_3H_5)(CO)$_2$(2,2′-bpy)Br] (0.215 g, 0.5 mmol), Tl[PF_6] (0.175 g, 0.5 mmol) and bipyridylethylene (BPE) (0.046 g, 0.25 mmol) in acetone (50 ml) was refluxed under nitrogen during 3 h. The red solution was filtered and the TlBr precipitate was washed several times with small amounts of acetone until it became white. The solution was evaporated under vacuum until dryness and was washed three times with EtOH. The precipitate was recrystallized from CH_2Cl_2–ether. Single crystals suitable for XRD were obtained by diffusion of ether into a concentrated CH_2Cl_2 solution of the complex.

Anal. Calc: C, 43.09; H, 3.10; N, 7.18. Found: C, 42.18; H, 3.36; N, 7.72%.

IR (KBr, cm^{-1}): 1947, 1857 ($\nu_{C\equiv O}$).

4.4. Synthesis of [Mo(η^3-C_3H_5)(CO)$_2$(2,2′-bpy)(4-CNpy)][PF_6] (4)

A suspension of [Mo(η^3-C_3H_5)(CO)$_2$(2,2′-bpy)Br] (0.215 g, 0.5 mmol), Tl[PF_6] (0.175 g, 0.5 mmol) and 4-cyanopyridine (0.026 g, 0.25 mmol) in acetone (20 ml) was refluxed under nitrogen during 3 h. The red solution was filtered and the TlBr precipitate was washed several times with small amounts of acetone until it became white. The solution was evaporated under vacuum until dryness and was washed three times with EtOH. The precipitate was recrystallized from CH_2Cl_2–ether. Single crystals suitable for XRD were obtained by diffusion of ether into a concentrated CH_2Cl_2 solution of the complex.

Anal. Calc: C, 42.16; H, 2.86; N, 9.36%. Found: C, 41.21; H, 2.98; N, 10.20%.

IR (KBr, cm^{-1}): 1948, 1857 ($\nu_{C\equiv O}$).

^{1}H-NMR (CD_3CN, 500 MHz), δ: 1.48 (d, *anti*-I), 1.60 (d, *anti*-II), 3.20 (m, *meso*-II), 3.40 (d, *syn*-II),3.60 (br, *syn*-I), 4.05 (m, *meso*- I), 7.58 (m, bpy H-5), 7.7 (m, bpy′ H-5), 7.7 (m[a], CNpy), 8.14 (m, bpy H-4), 8.16 (m, bpy′ H-4), 8.31 (d, bpy H-3), 8.37 (d, bpy′ H-3), 8.78 (m[a], CNpy), 8.81 (d, bpy H-6), 9.1 (br bpy′, H-6);); [a] part of a $(AB)_2$ system.

^{13}C-NMR (HMQC in CD_3CN), δ: 58.8 (*anti*-II), 59.3 (*anti*-I) 59.3 (*syn*-II), 60.0 (*syn*-I), 72.2 (*meso*-II), 74.5 (*meso*-I), 120.3 (bpy III-3), 120.5 (bpy′ III-3), 126.5 (CNpy), 127.3 (bpy III-5), 127.6 (bpy′ III-5), 140.5 (bpy III-4, bpy′ III-4), 151.0 (CNpy), 154.0 (bpy III-6), bpy′ III-6 not detected.

4.5. Synthesis of [Mo(η^3-C_3H_5)(CO)$_2$(2,2′-bpy)(4-Mepy)][PF_6] (5)

A suspension of [Mo(η^3-C_3H_5)(CO)$_2$(2,2′-bpy)Br] (0.430 g, 1 mmol), Tl[PF_6] (0.350 g, 1 mmol) and 4-Mepy (0.093 g, 1 mmol) in acetone (20 ml) was refluxed under nitrogen during 5 h. The red solution was filtered and the TlBr precipitate was washed several times with small amounts of acetone until it became white. The solution was evaporated under vacuum until dryness and was washed three times with EtOH. The precipitate was recrystallized from CH_2Cl_2–ether. Single crystals suitable for XRD were obtained by diffusion of ether into a concentrated CH_2Cl_2 solution of the complex.

Anal. Calc: C, 42.95; H, 3.43; N, 7.15. Found: C, 42.49; H, 3.43; N, 7.62%.

IR (KBr, cm^{-1}): 1939, 1865 ($\nu_{C\equiv O}$).

^{1}H-NMR (CD_3CN), δ: 1.50 (d, *anti*-I), 1.56 (d, *anti*-II), 1.66 (d, *anti*-III), 2.10 (s, CH_3), 2.16 (s, CH_3), 2.27 (s, CH_3), 3.15 (m, *meso*-II), 3.35 (m, *meso*-III), 3.37 (d, *syn*-II), 3.45 (d, *syn*-III), 3.53 (d, *syn*-I), 3.98 (m, *meso*-I), 6.90 (m[a], py), 7.03 (m[a], py), 7.14 (m[a], py), 7.65 (m, bpy+py), 7.89 (m[a], py),8.1 (m, bpy), 8.25 (m, bpy), 8.34 (m[a], py), 8.77 (d, bpy H-6), 9.03 (d, bpy H-6), 9.2 (br, bpy H-6); [a] part of a $(AB)_2$ system.

4.6. Synthesis of [{Mo(η^3-C_3H_5)(CO)$_2$(4,4′-dimethyl-2,2′-bpy)}$_2$(μ-pyrazine)][PF_6]$_2$ (6)

A suspension of [Mo(η^3-C_3H_5)(CO)$_2$(4,4′-dimethyl-2,2′-bpy)Br] (0.230 g, 0.5 mmol), Tl[PF_6] (0.175 g, 0.5 mmol) and pyrazine (0.02 g, 0.25 mmol) in acetone (50 ml) was refluxed under nitrogen during 5 h. The red solution was filtered and the TlBr precipitate was washed several times with small amounts of acetone until it became white. The solution was evaporated under vacuum until it dried and was washed three times with Et_2O. The precipitate was recrystallized from Et_2O–hexane.

Anal. Calc: C, 40.59; H, 3.41; N, 7.47. Found: C, 40.64; H, 3.66; N, 8.00%.

IR (KBr, cm^{-1}): 19442, 1878 ($\nu_{C\equiv O}$).

^{1}H-NMR (CD_3CN), δ: 1.46 (d, *anti*-I), 1.52 (d, *anti*-II), 2.44 (s, CH_3), 2.48 (s, CH_3) 3.1 (m, *meso*-II), 3.32 (d, *syn*-II), 3.50 (d, *syn*-I), 3.95 (m, *meso*-I), 7.38 (d, bpy H-5), 7.50 (d, bpy′ H-5), 8.10 (s, bpy H-3), 8.17 (s, bpy′ H-

3), 8.48 (s, pyrazine), 8.64 (d, bpy H-6), 9.0 (br, bpy′ H-6).

Single crystals suitable for XRD were obtained by diffusion of ether into a concentrated CH_2Cl_2 solution of the complex, leading to another complex (**7**).

4.7. Synthesis of [{Mo(η³-C₃H₅)(CO)₂(4,4′-dimetyl-2,2′-bpy)(NCMe)}][PF₆] (7)

A suspension of $[Mo(\eta^3\text{-}C_3H_5)(CO)_2(NCMe)_2Br]$ (0.355 g, 1 mmol), Tl[PF_6] (0.349 g, 1 mmol) and 4,4′-dimethyl-2,2′-bpy (0.184 g, 1 mmol) in acetone (20 ml) was refluxed under nitrogen during 5 h. The orange solution was filtered and the TlBr precipitate was washed several times with small amounts of acetone until it became white. The solution was evaporated under vacuum until it dried and was washed three times with Et_2O. The orange precipitate was recrystallized from CH_2Cl_2/EtOH.

Anal. Calc: C, 40.51; H, 3.58; N, 7.46. Found: C, 40.30; H, 3.14; N, 7.45%.

IR (KBr, cm^{-1}): 1941, 1853 ($\nu_{C\equiv O}$).

4.8. Synthesis of [{Mo(η³-C₃H₅)(CO)₂(4,4′-dimethyl-2,2′-bpy)Br] (8)

A suspension of $[Mo(\eta^3\text{-}C_3H_5)(CO)_2(NCMe)_2Br]$ (0.355 g, 1 mmol) and 4,4′-dimethyl-2,2′-bpy (0.184 g, 1 mmol) was stirred in EtOH (10 ml) under nitrogen during 5 h. The orange precipitate was filtered, washed several times with small amounts of EtOH, and dried under vacuum. Single crystals suitable for XRD were obtained by diffusion of ether into a concentrated CH_2Cl_2 solution of the complex.

Anal. Calc: C, 44.66; H, 3.75; N, 6.13. Found: C, 44.52; H, 3.39; N, 6.19%.

IR (KBr, cm^{-1}): 1941, 1853 ($\nu_{C\equiv O}$).

5. Crystallography

The pertinent crystallographic parameters for complexes **2**–**5**, **7** and **8** are summarized in Table 3. X-ray data were collected at room temperature on a MAR research plate system using graphite monochromatized Mo–K_α radiation ($\lambda = 0.71073$ Å) at Reading University. The crystals were positioned at 70 mm from the image plate. 95 frames were taken at 2° intervals using a counting time adequate to the crystal under study. Data analysis was performed with the XDS program [11]. Intensities of complexes **3** and **8** were corrected empirically for absorption effects, using a DIFABS version modified for image plate geometry [12]. No absorption correction was applied to the intensities of the remaining complexes.

Structures were solved by direct methods and by subsequent difference Fourier syntheses and refined by full-matrix least-squares on F^2 using the SHELX-97 system programs [13]. All non-hydrogen atoms were refined giving anisotropic thermal parameters except the fluorine atoms in complexes **7** and **5**, which were refined with individual isotropic thermal parameters. In these two cases, the PF_6^- anions were included in the refinement considering two alternative octahedral sites with refined occupation factors of x and $1-x$, x being equal to 0.64(2) in **5** and 0.74(1) in **7**. In complexes **3** and **5** the oxygen atom of the solvent water molecule was refined with isotropic temperature factor and with an occupation factor set to 0.50, in order to give a reasonable thermal parameter.

The hydrogen atoms on the parent carbon atoms were included in calculated positions and given thermal parameters equivalent 1.2 times those of the atom to which they were attached. In complexes **3** and **5**, the hydrogen atoms of the water molecules were not revealed by the successive Fourier maps and their positions were not introduced in the refinement. In the last difference Fourier map calculated for complex **8**, the highest peak had an electronic density of 2.40 e $Å^{-3}$, which was within molybdenum coordination sphere. Complex **3** was composed of ca. 50% of crystal and ca. 50% of powder and gave very poor diffraction patterns leading undoubtedly to a structure with poor quality. However, it was possible to locate all non-hydrogen atoms of complex, the counter-ions as well as two solvent molecules: one MeCN and one water molecule. The final Fourier map showed a peak with an electronic density of 2.38 e $Å^{-3}$ situated at 2.20 Å from a carbon atom of the BPE bridge. All attempts to assign this peak lead to unstable trial models and the structure presented represents the model with chemical significance and lower R value. For the remaining complexes the residual electronic density was within the expected values.

6. Supplementary material

Crystallographic data for the structural analyses have been deposited with the Cambridge Crystallographic Data Centre, CCDC nos. 213037 (**2**), 213038 (**3**), 213039 (**4**), 213040 (**5**), 213041 (**7**), and 213042 (**8**). Copies of this information may be obtained free of charge from The Director, CCDC, 12 Union Road, Cambridge CB2 1EZ, UK (Fax: +44-1223-3336033; e-mail: deposit@ccdc.cam.ac.uk or www: http://www.ccdc.cam.ac.uk).

Table 3
Room temperature crystal data and pertinent refinement details for complexes **2**–**5**, **7**, and **8**

Complex	**2**	**3**	**4**	**5**	**7**	**8**
Formula	$C_{40}H_{34}F_{12}Mo_2N_6O_4P_2$	$C_{45}H_{40}F_{12}Mo_2N_6O_{4.5}P_2$	$C_{21}H_{17}F_6MoN_4O_2P$	$C_{21}H_{20}F_6MoN_3O_{2.5}P$	$C_{19}H_{20}F_6MoN_3O_2P$	$C_{17}H_{17}BrMoN_2O_2$
M_w	1144.55	1218.65	598.30	595.31	563.29	457.18
Crystal system	Monoclinic	Triclinic	Monoclinic	Monoclinic	Orthorhombic	Monoclinic
Space group	$P2_1/n$	$P\bar{1}$	$P2_1/n$	$C2/c$	$Pn2_1a$	$Pna2_1$
a (Å)	7.938(9)	11.327(14)	10.729(11)	28.396(29)	12.266(13)	8.144(11)
b (Å)	11.525(13)	13.857(17)	14.915(15)	12.672(14)	13.326(14)	12.132(13)
c (Å)	30.642(32)	17.168(23)	15.366(16)	15.648(17)	13.965(14)	17.895(21)
α (°)	(90)	85.90(1)	(90)	(90)	(90)	(90)
β (°)	93.98(1)	81.50(1)	106.45(1)	114.60(1)	(90)	95.49(1)
γ (°)	(90)	83.22(1)	(90)	(90)	(90)	(90)
V (Å^3)	2796	2642	2358	5120	2283	1760
Z	2	2	4	8	4	4
D_c (Mg m^{-3})	1.359	1.532	1.685	1.545	1.639	1.725
μ (mm^{-1})	0.584	0.624	0.698	0.643	0.714	3.025
Reflections collected	8165	16323	7674	6965	7190	5650
Unique reflections (R_{int})	4955, [0.0947]	9367, [0.1351]	4267, [0.0730]	4316, [0.1006]	4259, [0.0879]	3091, [0.0553]
Final R indices						
R_1, wR_2 [$I > 2\sigma(I)$]	0.1154, 0.3403	0.1315, 0.2916	0.0798, 0.1833	0.1102, 0.3104	0.0897, 0.2171	0.0800, 0.2315
R_1, wR_2 (all data)	0.1592, 0.3588	0.1948, 0.3094	0.1337, 0.2101	0.1880, 0.3520	0.1661, 0.2510	0.1246, 0.2570

Acknowledgements

This work was supported by PRAXIS XXI under project PRAXIS/PCNA/C/QUI/103/96. A joint travel grant by the Deutscher Akademischer Austauschdienst and Conselho de Reitores das Universidades Portuguesas (“Acções Integradas Luso-Alemãs”, A-10/01) to M.J.C. and H.W. is gratefully acknowledged. P.M.F.J.C. and M.J.C. acknowledge the TMR Metal Clusters in Catalysis and Organic Synthesis. V.F. and M.G.B.D. thank the EPSRC (U.K.) and the University of Reading for funds for the Image Plate system.

References

[1] (a) J.M. Lehn, Angew. Chem. Int. Ed. Engl. 29 (1990) 1304;
(b) D. Braga, F. Grepioni, Acc. Chem. Res. 27 (1994) 51;
(c) M.J. Calhorda, D. Braga, F. Grepioni, Transition metal clusters—the relationship between molecular and crystal structure, in: P. Braunstein, L.A. Oro, P.R. Raithby (Eds.), Metal Clusters in Chemistry, Wiley-VCH, Weinheim, 1999;
(d) D. Braga, F. Grepioni, A.G. Orpen (Eds.), Crystal Engineering: from Molecules to Crystals, to Materials, Kluwer Academic Publishers, Dordrecht, 1999.;
(e) Dalton Discussion 3: Inorganic Crystal Engineering, Bologna, 2000.

[2] (a) R.-D. Schnebeck, E. Freisinger, B. Lippert, Eur. J. Chem. (2000) 1193;
(b) R.K. Biradha, A. Mondal, B. Moulton, M.J. Zaworotko, J. Chem. Soc. Dalton Trans. (2000) 1.

[3] (a) H. tom Dieck, H. Friedel, J. Organomet. Chem. 14 (1968) 375;
(b) R.G. Hayter, J. Organomet. Chem. 13 (1967) P1;
(c) P.K. Baker, Adv. Organomet. Chem. 40 (1996) 45 (and references cited therein).

[4] (a) F. Dewans, J. Dewailly, J. Meunier-Piret, P. Piret, J. Organomet. Chem. 76 (1974) 53;
(b) F. Dewans, E. Goldenberg, Brevet d′Invention, Inst. Int. Prop. Indust. (1972) 2.120.573.

[5] (a) B.M. Trost, M.J. Lautens, Organometallics 2 (1983) 1687;
(b) B.M. Trost, M.J. Lautens, J. Am. Chem. Soc. 104 (1982) 5543;
(c) B.M. Trost, M.J. Lautens, J. Am. Chem. Soc. 105 (1982) 3343;
(d) B.M. Trost, M.-H. Hung, J. Am. Chem. Soc. 105 (1983) 7757.

[6] J.R. Ascenso, C.G. de Azevedo, M.J. Calhorda, M.A.A.F. de, C.T. Carrondo, P. Costa, A.R. Dias, M.G.B. Drew, V. Félix, A.M. Galvão, C.C. Romão, J. Organomet. Chem. 632 (2001) 197.

[7] (a) B.J. Brisdon, K.E. Paddick, J. Organomet. Chem. 149 (1978) 113;
(b) B.J. Brisdon, A.A. Wolf, J. Chem. Soc. Dalton Trans. (1978) 291;
(c) J.W. Faller, D.A. Haitko, R.D. Adams, D.F. Chodosh, J. Am. Chem. Soc. 99 (1978) 1654;
(d) J.W. Faller, D.H. Haitko, J. Organomet. Chem. 149 (1978) C19;
(e) B.J. Brisdon, M. Cartwright, J. Organomet. Chem. 164 (1979) 83;
(f) P. Espinet, R. Hernando, G. Iturbe, F. Villafañe, G. Orpen, I. Pascual, Eur. J. Inorg. Chem. (2000) 1031.

[8] (a) P. Pinto, E. Barranco, M.J. Calhorda, V. Félix, M.G.B. Drew, J. Organomet. Chem. 601 (2000) 34;
(b) H.D. Murdoch, R. Henzi, J. Organomet. Chem. 5 (1996) 552.

[9] (a) D. Morales, M.E.N. Clemente, J. Perez, L. Riera, V. Riera, D. Miguel, Organometallics 21 (2002) 4934;
(b) J. Perez, E. Hevia, L. Riera, V. Riera, S. Garcia-Grande, E. Garcia-Rodriguez, D. Miguel, Eur. J. Inorg. Chem. (2003) 1113.
[10] R.H. Fenn, A.J. Graham, J. Organomet. Chem. 37 (1972) 137.
[11] W. Kabsch, J. Appl. Crystallogr. 21 (1988) 916.
[12] N. Walker, D. Stuart, DIFABS, Acta Crystallogr. Sect. A 39 (1983) 158.
[13] G.M. Sheldrick, SHELX-97, University of Göttingen, Göttingen, Germany, 1997.